HYDRODYNAMIC AND MAGNETIC PAIRWISE INTERACTION OF PARTICLES IN SUSPENSIONS

Hugo Leonnardo Gomides do Couto
Universidade de Brasília, Departamento de Engenharia Mecânica
Campus Universitário Darcy Ribeiro, 70910-900, Brasília-DF, Brasil
hlcouto@unb.br

Francisco Ricardo da Cunha (corresponding author)
Universidade de Brasília, Departamento de Engenharia Mecânica
Campus Universitário Darcy Ribeiro, 70910-900, Brasília-DF, Brasil
frcunha@unb.br

Abstract. *This work concerns with a theoretical investigation of the pair-interacting of magnetic particles in a dilute sedimenting suspension. The suspension is composed of magnetic spherical particles of different radius and density immersed in a Newtonian fluid. The particles settle relative to one another under the action of gravity. When in close contact, the polarized particles may exert on each other an attractive van der Waals force and a magnetic force due to particle magnetization. The numerical simulations are based on direct computations of the hydrodynamic interactions among the rigid spheres in the regime of low particle Reynolds number. Depending on the relative importance of the interparticle forces and gravity, the collisions may result in aggregation or simply in a break of particle relative trajectory symmetry imposed by time reversibility. The rate at which aggregates are formed is calculated in order to evaluate suspension-stabilization by particle magnetization.*

Keywords: *sedimentation, hydrodynamic interaction, magnetic particles, aggregation, irreversibility.*

1. Introduction

In a dilute dispersion, the probability of a third sphere influencing the relative motion of two interacting particles is small, and so we only need consider binary interactions of particles. This relative motion, in sedimenting suspensions, is promoted by the different sizes and densities of the particles. If Brownian motion, inertia and interparticle forces are negligible, two spherical particles collide in a sedimenting dilute suspension in a reversible way returning to their initial streamlines. However, when the interparticle forces are significant, like in this study, the particles in close contact may exert on each other an attractive van der Waals force and a magnetic force due to particle magnetization. As a result of these forces, the particles are submitted to a lateral migration and hence the collisions may result in aggregation or simply in a break of particle relative trajectory symmetry imposed by time-reversibility.

The relative trajectories that not result in aggregation are used to determine dispersion of particles across the streamlines generated by the sources of irreversibility of the suspension under gravity or submitted to a shear flow. The migration of non-colloidal particles in a suspension give rise to a dispersive process which may be characterized as self-dispersion owing to the random of nature of collision among the suspended particles. The first experimental investigation were carried out by Eckstein, Bailey & Shapiro (1977), who determined the lateral shear-induced coefficient of self-dispersion of spherical particles in a Couette device. In subsequent studies, more accurate experiments for evaluating the self-dispersion coefficient are carried out by Leighton & Acrivos (1987). Acrivos et al. (1992) have calculated the component of the hydrodynamic diffusivity in the flow direction for a dilute suspension undergoing simple shear flow. In addition, Cunha & Hinch (1996) presented results for the transverse shear-induced self-diffusivity and gradient diffusivity in the direction of the velocity gradient for simple shearing of a dilute suspension of rough spheres and their theory has been extended by Loewenberg & Hinch (1997) to study self-dispersion of deformable drops. For a sedimenting suspension, the diffusivity has been determined for a heavy sphere falling through a dilute suspension of neutrally buoyant spheres by Davis & Hill (1992). Similar results were carried out by Davis (1992) for rough spheres. Two-particle relative trajectory are also presented by Couto, Abade & Cunha (2004) for the case when the van der Waals forces are relevant.

For the cases in which the aggregation occurs, the quantity of interest is the rate of doublet formation. The pioneer studies to estimate the rate of aggregation of a dispersion were developed by Smoluchowski (1917). In his model, the particles are submitted only to a sticking force on contact, i.e. without any hydrodynamic interaction or interparticle force. On the other hand, Zeichner & Schowalter (1977) included the effects of hydrodynamic interaction and interparticle force, computing the rate of aggregation of a dispersion of equal spheres subject to simple shear and to uniaxial extensional flow. Furthermore, Curtis & Hocking (1970) have performed a similar calculation for shear flows, and reported experimental results showing the importance of van der Waals forces in particle-aggregation. For gravity-induced aggregation of rigid spheres, Davis (1984) developed a theoretical model to investigate the influence of van der Waals and Maxwell slip in the collision efficiency. Using a boundary integral formulation, the interaction and the collision of two deformable

drops was computed by Loewenberg & Hinch (1997). At arbitrary Péclet numbers, using the full solution of the Fokker-Planck equation for the pair distribution of particles function Zinchenko & Davis (1992) evaluated the coalescence of drops induced by gravity. Moreover, Zinchenko & Davis (1994) and Cunha, Almeida & Lowenberg (2003) computed the collision rates of spherical drops in a shear flow.

In this paper we develop a theoretical calculation of the relative trajectories of pairwise interacting magnetic particles in a dilute sedimenting suspension with low particle Reynolds number. From the pairwise trajectories analysis the influence of particle magnetization on the rate of particle aggregation and the break of relative trajectory symmetry imposed by time-reversibility is examined for different conditions of the parameters that considers the relative importance between interparticle forces and gravity. We investigate the influence of the attractive van der Waals force and the magnetic interaction between two particle-dipoles as new sources of irreversibility for breaking symmetry after particle come into contact in creeping flows.

2. Formulation of the problem

Consider two rigid smooth magnetic particles of radius a_1 e a_2, densities ρ_1 e ρ_2 and magnetizations $\boldsymbol{M}_1 = M_1\hat{\boldsymbol{d}}_1$ and $\boldsymbol{M}_2 = M_2\hat{\boldsymbol{d}}_2$ immersed in a Newtonian fluid of density ρ and viscosity μ. A uniform gravitational force per unit mass $\boldsymbol{g} = -g\boldsymbol{e}_2$ acts on the dispersion. Fig. (1) shows a scheme of the pairwise particle interaction.

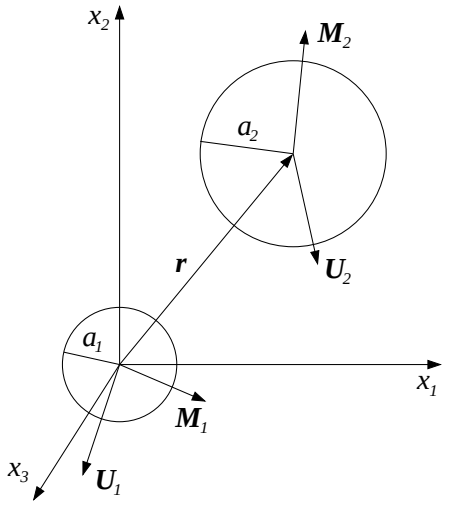

Figure 1. Schematic of the coordinate system used for the relative motion of two different-sized polarized particles.

The pairwise collision of particles are gravity-induced due to different particle radius and densities. The polydispersity of the pair of particles is characterized by the radius ratio λ and reduced densities ratio γ, defined as follows

$$\lambda \equiv \frac{a_2}{a_1} \qquad \text{and} \qquad \gamma \equiv \frac{\rho_2 - \rho}{\rho_1 - \rho}. \tag{1}$$

The centres of the particles 1 and 2 are located in $\boldsymbol{X}$ e $\boldsymbol{Y}$, respectively, where $\boldsymbol{r} \equiv \boldsymbol{X} - \boldsymbol{Y} = r\hat{\boldsymbol{r}}$ denotes the vector joining the centres of the two particles. Furthermore, the dimensionless distance is denoted by $s \equiv 2r/(a_1 + a_2)$. The settling velocities of a isolated particle of species i corresponds to the Stokes velocities $\boldsymbol{U}_i^{(0)} = 2a_i^2(\rho_i - \rho)\boldsymbol{g}/9\mu$, being $\boldsymbol{U}_2^{(0)} = \gamma\lambda^2\boldsymbol{U}_1^{(0)}$. The relative velocity due to gravity are defined by $\boldsymbol{U}_{12}^{(0)} \equiv \boldsymbol{U}_2^{(0)} - \boldsymbol{U}_1^{(0)}$, and its modulus $U_{12}^{(0)}$ will be used as a velocity scale of the motion.

We suppose that the particles are sufficiently small for inertial forces to be negligible in the particles and in the fluid. Then the particle Reynolds number $Re_i \equiv a_i U_i^{(0)}\rho/\mu$ $(i = 1, 2)$ is vanishingly small so that the Stokes equations are used in the formulation, namely

$$\nabla \cdot \boldsymbol{u} = 0 \qquad \text{and} \qquad \nabla \cdot \boldsymbol{\sigma} + \rho\boldsymbol{g} = \boldsymbol{0}. \tag{2}$$

Here, $\boldsymbol{u}$ is the Eulerian velocity field and $\boldsymbol{\sigma}$ the local Newtonian stress tensor, expressed by $\boldsymbol{\sigma} = -p\boldsymbol{I} + 2\mu\boldsymbol{E}$, where p denotes the pressure and $\boldsymbol{E}$ is the rate of strain tensor, defined as $\boldsymbol{E} \equiv (1/2)[(\nabla\boldsymbol{u}) + (\nabla\boldsymbol{u})^T]$.

It should be important to note that, in this work, we restrict our attention to dispersions where the Péclet number is large (negligible Brownian motion). This condition is represented by

$$\mathrm{Pe}_{12} \equiv \frac{1}{2}\frac{a_1 + a_2}{D_{12}^{(0)}} U_{12}^{(0)} \gg 1 \tag{3}$$

where $D_{12}^{(0)} \equiv (kT/6\pi\mu)(1/a_1 + 1/a_2)$ denotes the relative diffusivity due to Brownian motion.

2.1 Creeping flow solution in terms of mobility functions

Since the Stokes equations are linear and quasi-steady, the velocity of each sphere depends only on the instantaneous relative location of the two spheres, and is linear with respect to the applied forces, $\boldsymbol{F}_1$ and $\boldsymbol{F}_2$. Both spheres are torque free. Thus, the translational velocities $\boldsymbol{U}_1$ e $\boldsymbol{U}_2$ are determined by the following mobility relations (Kim & Karrila, 1991):

$$\begin{bmatrix} \boldsymbol{U}_1 \\ \boldsymbol{U}_2 \end{bmatrix} = \begin{bmatrix} \boldsymbol{b}_{11} & \boldsymbol{b}_{12} \\ \boldsymbol{b}_{21} & \boldsymbol{b}_{22} \end{bmatrix} \begin{bmatrix} \boldsymbol{F}_1 \\ \boldsymbol{F}_2 \end{bmatrix} \qquad \text{and} \qquad \boldsymbol{b}_{\alpha\beta} = \frac{1}{3\pi\mu(a_\alpha + a_\beta)} \left[A_{\alpha\beta} \frac{\boldsymbol{rr}}{r^2} + B_{\alpha\beta} \left(\boldsymbol{I} - \frac{\boldsymbol{rr}}{r^2} \right) \right], \tag{4}$$

where the square matrix is the global mobility, that contains the second order tensors $\boldsymbol{b}_{\alpha\beta}$ $(\alpha, \beta = 1, 2)$ and $\boldsymbol{I}$ denotes the unity second order tensor. The two-sphere mobility functions $A_{\alpha\beta}(s, \lambda)$ and $B_{\alpha\beta}(s, \lambda)$ depend only on λ and the dimensionless s. These functions are given in Appendix A. Numerical values of the mobility functions for arbritrary λ and s have been made available by Jeffrey & Onishi (1984) and Kim & Karrila (1991) to the near field and far field of particle configurations. It can be shown from the reciprocal theorem that these functions are unchanged when λ are replaced by the reciprocal λ^{-1} (Happel & Brenner,1967). Acting on the particles are the $\boldsymbol{F}_i$ force that includes the net weight, the attractive van der Waals force and the magnetic interaction force. Therefore, $\boldsymbol{F}_i$ is expressed in the following form

$$\boldsymbol{F}_i = \frac{4}{3}\pi a_i^3(\rho_i - \rho)\boldsymbol{g} + (2i-3)(\nabla\phi_A + \nabla\phi_M), \qquad i = 1, 2, \tag{5}$$

where ϕ_A and ϕ_M are the interparticle potentials of the van der Waals and magnetic forces, respectively.

2.2 Interparticle forces

2.2.1 van der Waals interaction

The van der Waals force between two particles was first calculated by Hamaker (1937). However, the Hamaker calculation neglected electromagnetic retardation and hence it is valid only for separations less than the London wavelength λ_ℓ, that is typically $0.1\mu m$ for hydrosol dispersions. This retardation effect was considered by Schenkel & Kitchener (1960) that proposed the following approximations:

$$\phi_A = \begin{cases} -\dfrac{A}{12\xi(1 + 11.2h/\lambda_\ell)} \dfrac{4\lambda}{(1+\lambda)^2}, & \text{when} \quad \dfrac{h}{\lambda_\ell} \leq \pi \\ -\dfrac{10^{-3}A}{\xi} \left\{ \dfrac{6.5}{h/\lambda_\ell} - \dfrac{0.305}{(h/\lambda_\ell)^2} + \dfrac{0.0057}{(h/\lambda_\ell)^3} \right\} \dfrac{4\lambda}{(1+\lambda)^2}, & \text{when} \quad \dfrac{h}{\lambda_\ell} > \pi \end{cases} \tag{6}$$

where A is the composite Hamaker constant and h is the gap between the particles. The dimensionless gap is expressed by ξ, so that $\xi = s - 2$. In Eq. (6) the term h/λ_ℓ can be expressed in an appropriated form showed below

$$\frac{h}{\lambda_\ell} = \left(\frac{2h}{a_\alpha + a_\beta} \right) \left(\frac{a_\alpha + a_\beta}{2\lambda_\ell} \right) = \xi \left(\frac{a_\alpha + a_\beta}{2\lambda_\ell} \right). \tag{7}$$

According to Eq. (6) the influence of electromagnetic retardation on the short-range potential interaction associated to van der Waals force is considered in our two-particle trajectories simulation. Thus, we define a retardation coefficient $\epsilon_R \equiv a_\alpha/\lambda_\ell$ obtaining the following expression

$$\frac{h}{\lambda_\ell} = \xi \frac{(1+\lambda)}{2} \epsilon_R. \tag{8}$$

For hydrosol dispersions the typical radii of a particle is $a_\alpha \sim 1\mu m$ and hence $\epsilon_R \equiv a_\alpha/\lambda_\ell \sim 10$.

2.2.2 Magnetic interaction

For the magnetic interaction between two dipoles, the far-field expression given in Rosensweig (1985) is used, namely

$$\phi_M = \frac{\mu_0 (M_1 V_1)(M_2 V_2)}{4\pi r^3} \left[\hat{\boldsymbol{d}}_1 \cdot \hat{\boldsymbol{d}}_2 - 3(\hat{\boldsymbol{d}}_1 \cdot \hat{\boldsymbol{r}})(\hat{\boldsymbol{d}}_2 \cdot \hat{\boldsymbol{r}}) \right]. \tag{9}$$

where $\hat{\boldsymbol{r}} \equiv \boldsymbol{r}/r$ is the unit vector along the line of centres of the particles, V_1 and V_2 are the particle volumes and μ_0 is the magnetic permeability of the free space and has the value $\mu_0 = 4\pi \times 10^{-7} H \cdot m^{-1}$. For the non-dimensionalizing Eqs. (6) and (9), we chosen A and $\mu_0 M_1^2 V_1$ as a measure of the strength of the van der Waals and magnetic forces, respectively. Then, Eq. (9) can be rewritten in a dimensionless form as being

$$\phi_M = \frac{M_{12}}{3s^3} \left(\frac{2\lambda}{1+\lambda} \right)^3 \left[\hat{\boldsymbol{d}}_1 \cdot \hat{\boldsymbol{d}}_2 - 3(\hat{\boldsymbol{d}}_1 \cdot \hat{\boldsymbol{s}})(\hat{\boldsymbol{d}}_2 \cdot \hat{\boldsymbol{s}}) \right], \tag{10}$$

where $M_{12} = M_2/M_1$ is the magnetization intensity ratio and the dimensionless distance vector are defined as $\hat{\boldsymbol{s}} \equiv \boldsymbol{s}/s$.

2.3 Relative trajectory governing equation

Since inertia forces are neglected in the present analysis, the equation of the motion of the two spheres consists in the balance between the hydrodynamic force on each particle and the applied force $\boldsymbol{F}_i$. Thus, the vector $\boldsymbol{s}$ time evolution, in a dimensionless form, is governed by the following differential equation

$$\frac{\mathrm{d}\boldsymbol{s}}{\mathrm{d}t} = \boldsymbol{U}_{12} \equiv \boldsymbol{U}_2 - \boldsymbol{U}_1. \tag{11}$$

By substituting (5) into (4), one obtains an expression for the relative velocity $\boldsymbol{U}_{12}$ that, in terms of dimensionless quantities, is given by

$$\boldsymbol{U}_{12} = \boldsymbol{g}\cdot\left[\frac{\boldsymbol{ss}}{s^2}L(s) + \left(\boldsymbol{I} - \frac{\boldsymbol{ss}}{s^2}\right)M(s)\right] - \left(\frac{\nabla\phi_A}{H_A} + \frac{\nabla\phi_M}{H_M}\right)\cdot\left[\frac{\boldsymbol{ss}}{s^2}G(s) + \left(\boldsymbol{I} - \frac{\boldsymbol{ss}}{s^2}\right)H(s)\right] \tag{12}$$

where $L(s)$, $M(s)$, $G(s)$ and $H(s)$ are scalar functions of s given by

$$L(s) = \frac{\gamma\lambda^2 A_{22} - A_{11}}{\gamma\lambda^2 - 1} + \frac{2(1-\gamma\lambda^3)A_{12}}{(\gamma\lambda^2-1)(1+\lambda)}, \qquad G(s) = \frac{\lambda A_{11} + A_{22}}{(1+\lambda)} - \frac{4\lambda A_{12}}{(1+\lambda)^2}, \tag{13}$$

$$M(s) = \frac{\gamma\lambda^2 B_{22} - B_{11}}{\gamma\lambda^2 - 1} + \frac{2(1-\gamma\lambda^3)B_{12}}{(\gamma\lambda^2-1)(1+\lambda)}, \qquad H(s) = \frac{\lambda B_{11} + B_{22}}{(1+\lambda)} - \frac{4\lambda B_{12}}{(1+\lambda)^2}. \tag{14}$$

Similarly, the functions $L(s)$, $M(s)$, $G(s)$ and $H(s)$ are unchanged when λ and γ are substituted by their reciprocals λ^{-1} and γ^{-1}. The two terms on right-hand side of (12) represent the contributions of gravity and interparticle forces to the particle relative motion, respectively. Their relative importance may be measured by the following physical parameters, H_A and H_M

$$H_A \equiv \frac{1}{2}\frac{(a_1+a_2)U_{12}^{(0)}}{D_{12}^{(0)}}\frac{kT}{A} \qquad \text{e} \qquad H_M \equiv \frac{1}{2}\frac{(a_1+a_2)U_{12}^{(0)}}{D_{12}^{(0)}}\frac{kT}{\mu_0 M_1^2 V_1}. \tag{15}$$

Using Eq. (15) with $D_{12}^{(0)}$ definition we can obtain that $H_A = (6\pi\mu a_1 a_2 U_{12}^{(0)})/A$. This parameter can be interpreted as a relation between two energy scales; one associated with the work done by the viscous forces and other with the potential energy of the attractive van der Waals force represented by the Hamaker constant A. Similarly, the parameter $H_M = (6\pi\mu a_1 a_2 U_{12}^{(0)})/\mu_0 M_1^2 V_1$ can be seen as a measure of the relative importance between the work done by the viscous forces and the magnetic potential associated to the dipole-dipole interaction.

3. Numerical results

The governing equations for the relative trajectories of two interacting particles were integrated by using a fourth-order Runge-Kutta scheme. The asymptotic forms of the mobility functions for widely separated spheres given by Jeffrey & Onishi (1984) were used for $s > 2.3$. Otherwise, the near field mobilities giving by the same authors were used. Several time scales are involved in this computations and so particle overlapping needed to be avoided. We then use an adaptative time-step which takes into account the relative distance of the particles. To make a prediction for the smaller time-steps it is considered the balance between lubrication and the interparticle forces for the particles at closing contact. According to Cunha (2003) and Kim & Karrila (1991), the typical scales for the lubrication and the van der Waals forces are given by $6\pi\mu\bar{a}^2 U_\ell/h$ and $A\bar{a}/h^2$, respectively. Here, U_ℓ is a velocity scale associated with the lubrication and $\bar{a} = (a_1+a_2)/2$ a typical length scale of the relative motion. Similarly, we consider that $\mu_0 M^2 V\bar{a}/h^2$ is a typical scale for the magnetic interaction force. Therefore, we obtain the following balances at near particle-contact region.

$$\frac{6\pi\mu\bar{a}^2 U_\ell}{h} \sim \frac{A\bar{a}}{h^2} \qquad \text{and} \qquad \frac{6\pi\mu\bar{a}^2 U_\ell}{h} \sim \frac{\mu_o M^2 V\bar{a}}{h^2}. \tag{16}$$

Considering $t_\ell \sim \bar{a}/U_\ell$ a time scale associated with the lubrication and non-dimensionalizing this time using the typical settling time scale $t_s \sim \bar{a}/U_{12}^{(0)}$ we obtain the typical time-step used in our simulations

$$\delta t = \frac{1}{10}\min\left\{10^{-2}, \xi^2 H_A, \xi^2 H_M\right\}. \tag{17}$$

Using this scheme, the errors in the numerical integration were less than 10^{-3}.

3.1 Typical relative trajectories

The particle migration explored here is governed by six dimensionless parameters. Thus, we have examined of each one on the particle relative trajectory. The gravity direction are indicated in all the figures by the $\boldsymbol{g}$ vector. The circle plotted with the relative trajectories represents the collision surface, whose radius is the sum of the particles radii, given by $a_1 + a_2$. Figs. (2) and (3) show the relative trajectories of particles under action of gravity in the presence of attractive van der Waals forces, for $H_M \gg 1$. Fig. (2.a) presents the results of trajectories for different initial conditions $x_1^{-\infty}$. We identify a critical value for $x_1^{-\infty}$, so that for values of $x_1^{-\infty}$ below than the critical distance $x_1^{-\infty} \leq x_c^*$, the trajectories always results in aggregation. Otherwise, for $x_1^{-\infty} > x_c^*$ the trajectories are opened only. For $\lambda = 0.5$, $\gamma = 1.0$ and $H_A = 0.01$, shown in Fig. (2.a), the critical value obtained was $x_c^* \cong 1.37$. For smaller values of $x_1^{-\infty} \leq x_c^*$ the point of collision occurs in smaller angle on particle surface, implying in shorter closed trajectories before collision (i.e. shorter times for collision).

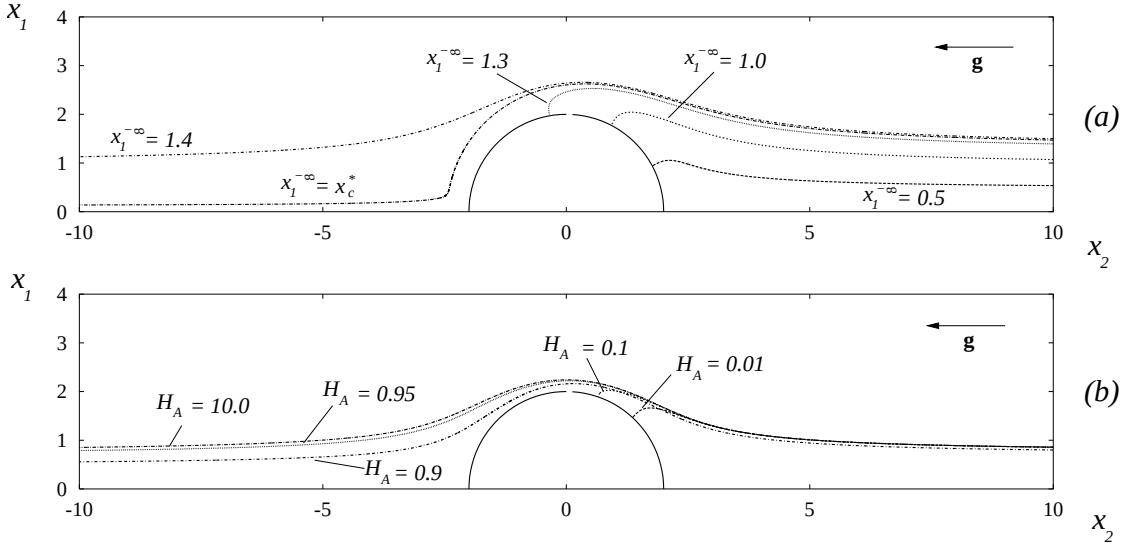

Figure 2. The influence of the physical parameters on the relative trajectories of the particles. (a) Effect of the initial condition $x_1^{-\infty}$ for $\lambda = 0.5$, $\gamma = 1.0$ and $H_A = 0.01$; (b) Different values of the van der Waals parameter H_A for $x_1^{-\infty} = 0.8$, $\lambda = 0.5$ and $\gamma = 1.0$.

In addition, the effect of the parameter H_A on the particle trajectories is shown in Fig. (2.b). For $x_1^{-\infty} = 0.8$, $\lambda = 0.5$ e $\gamma = 1.0$, when $H_A = 0.01$ or 0.1 the collision between the particles occurs, because the van der Waals force dominates the gravity action and the viscous interactions due to lubrication. On other hand, for $x_1^{-\infty} = 0.8$, $\lambda = 0.5$ e $\gamma = 1.0$ $H_A = 10.0$ the particle pass through the other following a reversible trajectory. Between these two limits for H_A, an important phenomena is also identified; the break of the particle relative trajectory time-reversibility, that represents a lateral particle displacement without formation of doublets of particles.

In order to evaluate the polydispersity effect on the net transversal displacement we need to consider the radius ratio λ and the reduced densities ratio γ. Fig. (3.a) shows that for increasing λ the probability for an eventual collision to occurs decreases. For $\lambda = 0.5$ and $x_1^{-\infty} = 1.5$, $\gamma = 1.0$, $H_A = 0.01$ the relative trajectory are irreversible, resulting in collision. However, for $\lambda = 0.25$ or 0.125, the particle pass through the other producing irreversible two-particle trajectories, but, in this case, these trajectories are opened. From the Fig. (3.b), we see that when γ increases, the relative velocities increases, dominating the attractive forces. For $x_1^{-\infty} = 1.2$, $\lambda = 0.5$, $H_A = 0.01$, the trajectories plotted for $\gamma \leq 1.5$ are all aggregative. However, for $\gamma = 1.9$ the two-particle trajectory are irreversible and opened. In particular, for $\gamma = 2.0$ the effect of van der Waals is negligible, resulting in a reversible opened relative trajectory.

Now, we show some results of relative particle trajectories for the case in which pairwise magnetic interaction is present in the suspension. The van der Waals forces are negligible, i.e., $H_A \gg 1$. For characterization of the magnetic aggregation three additional physical parameters are considered. Fig. (4.a) depicts the influence of the magnetization intensity ratio M_{12} on the relative particle trajectories. From these plot we can see that an increasing in the magnetization rate M_{12} of the particles may lead to a rapid coagulation. The Fig. (4.a) shows that for $\lambda = 0.5$, $\gamma = 1.0$, $x_1^{-\infty} = 2.5$, $\hat{\boldsymbol{d}}_1 = \hat{\boldsymbol{d}}_2 = (1, 0, 0)$, $H_M = 0.01$ and $M_{12} = 1.0$ and 0.75 the relative particle trajectories collide whereas for $M_{12} = 0.5$ the trajectory even not being aggregative is strong irreversible as can be seen by the no null net transversal displacement. This trajectory configuration is an indicative that a magnetic-induced diffusion arises in the flow suspension of magnetic particles even at dilute regimes in which pairwise interactions dominates. The value of $M_{12} = 0.25$ however produces only a slightly irreversible trajectory.

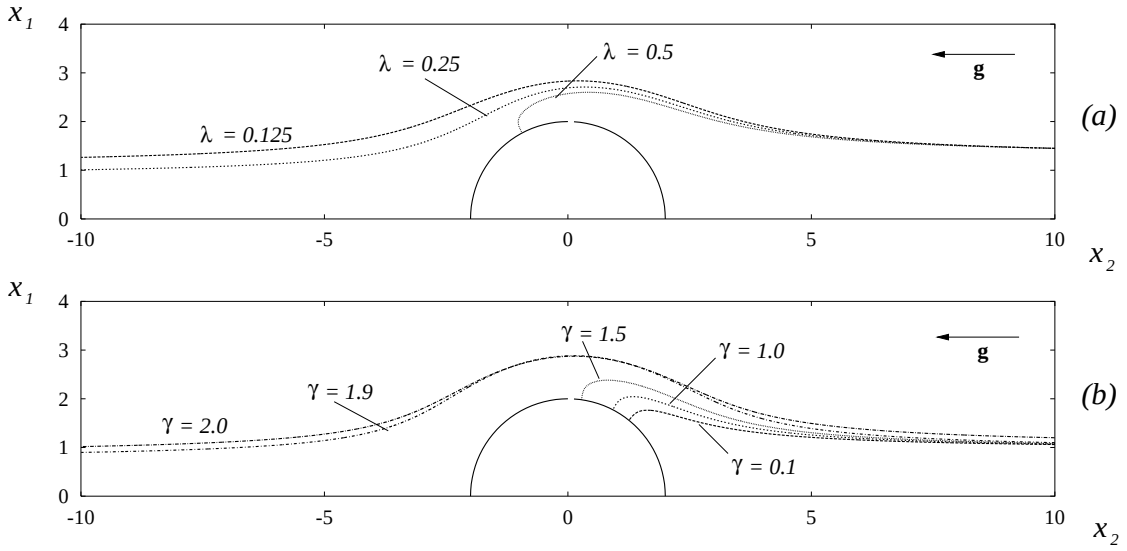

Figure 3. Influence of the physical parameters in two-particle relative trajectory. (a) Variations with the radius ratio λ for $x_1^{-\infty} = 1.5$, $\gamma = 1.0$ e $H_A = 0.01$; (b) Variations with the reduced densities ratio γ para $x_1^{-\infty} = 1.2$, $\lambda = 0.5$, $H_A = 0.01$.

Figure (4.b) shows the results of the influence of the potential magnetic interaction parameter, H_M. For $\lambda = 0.5$, $\gamma = 1.0$, $x_1^{-\infty} = 2.0$, $M_{12} = 1.0$, $\hat{\boldsymbol{d}}_1 = \hat{\boldsymbol{d}}_2 = (1, 0, 0)$. For the lower value $H_M = 0.01$ we note that aggregative closed trajectories occurs. In contrast, for $H_M = 0.1$ and 1.0 the relative trajectories are irreversible. This suggests that two magnetic particle encounters can lead to a gravity-induced diffusion produced by the magnetization effect of the particles. Only for high values of the magnetic parameter $H_M = 10.0$ the relative trajectory are foun to be fully reversible. Comparing these results with those shown in the Fig. (2.b), we can argue that the gravity-induced diffusion arising from magnetic interaction produces net transversal displacement at two order of magnitude greater than the ones arising from the the van der Waals attraction under the same physical conditions. This indicates that the relative particle trajectories tends to be more diffusive rather than aggregative in a suspension of magnetic particles undergoing a settling motion. Otherwise, we can conclude that the two-particle trajectories tends to be more aggregative when these particles are attracted by the van der Waals forces.

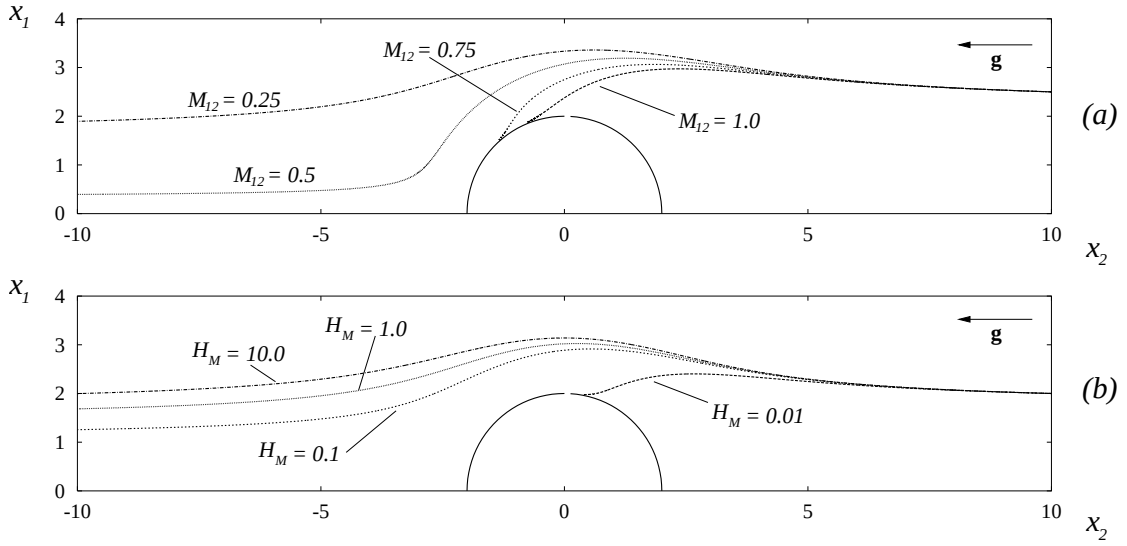

Figure 4. Relative trajectories of pairwise interacting magnetic particles. Influence of the physical magnetic parameters in the net transversal displacement. (a) Magnetization intensity ratio M_{12} for $\lambda = 0.5$, $\gamma = 1.0$, $x_1^{-\infty} = 2.5$, $\hat{\boldsymbol{d}}_1 = \hat{\boldsymbol{d}}_2 = (1, 0, 0)$ and $H_M = 0.01$; (b) The parameter of magnetic aggregation H_M para $\lambda = 0.5$, $\gamma = 1.0$, $x_1^{-\infty} = 2.0$, $M_{12} = 1.0$, $\hat{\boldsymbol{d}}_1 = \hat{\boldsymbol{d}}_2 = (1, 0, 0)$.

As exposed in the Eq. (9) the magnetic interaction force between two magnetic dipoles can be both attractive and repulsive natures, depending on the magnetization directions $\hat{\boldsymbol{d}}_1$ e $\hat{\boldsymbol{d}}_2$. Thus, some simulation results showing the effect

of the magnetization orientation on the two-particle encounters is presented in Fig. (5), for different configurations.

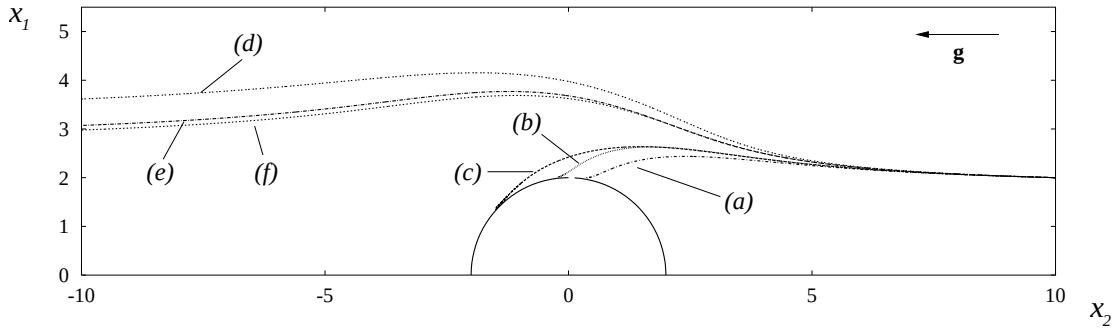

Figure 5. Effect of the magnetization orientation on the two-particle trajectories for $H_M = 0.01$, $\lambda = 0.5$, $\gamma = 1.0$, $x_1^{-\infty} = 2.0$ and $M_{12} = 0.5$. Particles oriented in the same directions (a) $\hat{\boldsymbol{d}}_1 = \hat{\boldsymbol{d}}_2 = (1, 1, 0)$; (b) $\hat{\boldsymbol{d}}_1 = \hat{\boldsymbol{d}}_2 = (0, 1, 0)$; (c) $\hat{\boldsymbol{d}}_1 = \hat{\boldsymbol{d}}_2 = (1, 0, 0)$. Particles oriented in opposed directions (d) $\hat{\boldsymbol{d}}_1 = -\hat{\boldsymbol{d}}_2 = (1, 1, 0)$; (e) $\hat{\boldsymbol{d}}_1 = -\hat{\boldsymbol{d}}_2 = (0, 1, 0)$; and (f) $\hat{\boldsymbol{d}}_1 = -\hat{\boldsymbol{d}}_2 = (1, 0, 0)$.

We see that for $H_M = 0.01$, $\lambda = 0.5$, $\gamma = 1.0$, $x_1^{-\infty} = 2.0$ and $M_{12} = 0.5$ and $\hat{\boldsymbol{d}}_1 = -\hat{\boldsymbol{d}}_2 = (1, 1, 0)$ corresponding to the condition of the opened trajectory (d) the net transversal displacement is approximately two orders of magnitude greater than the values obtained with configurations (e) and (f). This finding indicates that particle dipoles oriented in opposed direction such described in (d) produces several diffusive opened trajectories, and it would be the most important situation for producing mixing in the suspension. On the other hand the case (a), corresponding to particle dipoles oriented in the same direction with $\hat{\boldsymbol{d}}_1 = \hat{\boldsymbol{d}}_2 = (1, 1, 0)$, produces particle encounter after a time shorter than corresponding times for collision observed from the closed trajectories shown for the cases (b) and (c). The plots of Fig. (5) show that the potential forces generated by interacting magnetic particles in a suspension may have an important role for controlling irreversible particle flocculation in order to guarantee the processing of stable suspension

4. Collision efficiencies

The collision rate J_{12} is the flux of pairs into the collision surface $a_1 + a_2$ and is expressed by Davis (1984) and Zinchenko & Davis (1992) as

$$J_{12} = -n_1 n_2 \int_{r=a_1+a_2} p(\mathbf{r})\, \mathbf{U}_{12} \cdot \mathbf{n}\, dA \tag{18}$$

where n_i is the density number of the particle i and $p(\mathbf{r})$ is the pair-distribution function, that satisfies, in the dilute limit, the quasi-steady Fokker-Planck type equation $\nabla \cdot (p(\mathbf{r})\mathbf{U}_{12}) = 0$. In the inner boundary condition, we shall assume that the colliding spheres aggregate upon contact (no subsequent separation occurs) and the absence of far-field correlations yields the outer boundary condition. Mathematically, these conditions are expressed as follows

$$p(\mathbf{r}) = 0 \qquad \text{for} \quad r = a_1 + a_2 \qquad \text{and} \qquad p(\mathbf{r}) \to 1 \qquad \text{for} \qquad r \to \infty \tag{19}$$

The integral in Eq. (18) is taken over the surface which encloses the volume occupied by all the trajectories that originate at $r = \infty$ and terminate with the particles coming into contact. The cross section of this volume at $r = \infty$ is a circle with radius x_c^*, and, since, $p = 1$ and $\boldsymbol{U}_{12} = \boldsymbol{U}_{12}^{(0)}$ at $r = \infty$, the rate of doublet formation is then

$$J_{12} = n_1 n_2\, U_{12}^o\, \pi (a_1 + a_2)^2\, E_c, \tag{20}$$

where $E_c = x_c^*/(a_1 + a_2)^2$ is the collision efficiency. $E_c = 1.0$, corresponds to the ideal model proposed by Smoluchowski (1917) where the particles are assumed to move without hydrodynamic and interparticle interaction.

The problem here is reduced to the one of computing the parameter x_c^* which is the largest horizontal displacement from the vertical axis of symmetry ($\boldsymbol{g}$ is in the vertical direction) possible for two widely separated particles eventually collide. In Fig. (6) shows evaluated the effect of polydispersity on the collision efficiency for non-magnetic particles, i.e. $H_M \gg 1$. We see that, for larger values of γ, the collision efficiency are reduced significantly. This effect is clearly seen in the (c) curve, that for $\lambda = 0.5$, $\gamma = 2.0$ and $H_A = 100$ the collision efficiency is $E_c \cong 10^{-4}$.

The appreciable difference between the values of E_c for different λ was first observed by Adler (1981) for aggregation in shear flows and by Davis (1984) in sedimenting suspensions. In the plot of Fig. (6) the collision efficiency for $\lambda = 0.5$, $\gamma = 1.0$ and $H_A = 100$ is about three times greater than the corresponding value of E_c for $\lambda = 0.25$, $\gamma = 1.0$ and $H_A = 100$.

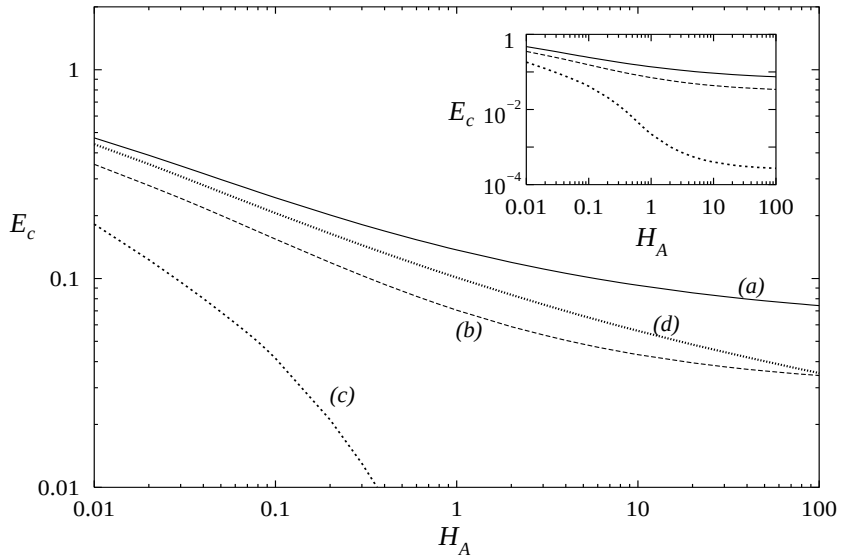

Figure 6. The collision efficiency as a function of the parameter H_A for the cases: (a) $\lambda = 0.5$ e $\gamma = 1.0$; (b) $\lambda = 0.5$ e $\gamma = 1.5$; (c) $\lambda = 0.5$ e $\gamma = 2.0$; e (d) $\lambda = 0.25$ e $\gamma = 1.0$. The insert shows the curve (c), not detailed in the main plot.

In a suspension, when the repulsive force dominates, the particles remain dispersed, and the dispersion is said to be stable; when the attractive forces dominate, the dispersion is unstable and the particles flocculate (Davis, 1984). As observed previously, the magnetic interaction force can be used as a repulsive force in order to promote the stabilization of the suspension, avoiding the doublet formation. According to the Fig. (7), this effect may be significant. We note that the collision efficiency can be reduced, for the limit $H_A = 100$, in 80% for the case (c), where $\lambda = 0.5$, $\gamma = 1.0$, $\hat{\boldsymbol{d}}_1 = \hat{\boldsymbol{d}}_2 = (1, 0, 0)$, $H_M = 0.1$ and $M_{12} = 1.0$, when compared with the case (a) under the same conditions but in the absence particle magnetization. This finding may be of interest in processes of magnetic separation, when non-magnetic particles are captured using magnetic carries (Stratulat et al., 2000), or in environmental processes that use the magnetic particles to remediation of oil spills (Sobral & Cunha, 2005).

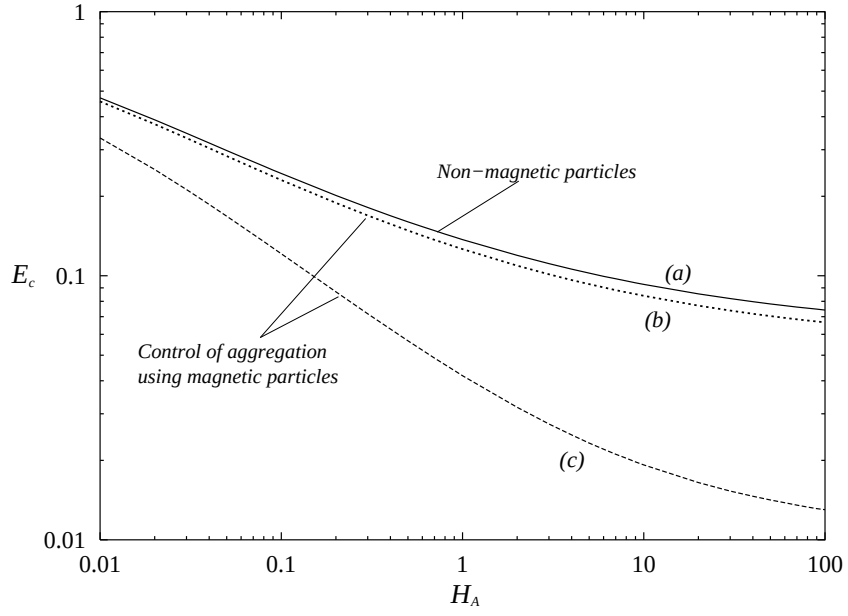

Figure 7. Analysis of the influence of magnetic particles in the dispersion on the collision efficiency for $\lambda = 0.5$, $\gamma = 1.0$, $\hat{\boldsymbol{d}}_1 = \hat{\boldsymbol{d}}_2 = (1, 0, 0)$: (a) $H_M \gg 1$ (non-magnetic particles); (b) $H_M = 1.0$ and $M_{12} = 1.0$; and (c) $H_M = 0.1$ and $M_{12} = 1.0$.

5. Reversibility diagrams

In practice a number of effects are able to break the symmetry of the relative particle trajectories imposed by the time reversibility of creeping flow; small amount of particle roughness (Cunha & Hinch, 1996; Davis, 1992), particle deformation (Loewenberg & Hinch, 1997), particle inertia (Davis, 1984) and the presence of interparticle forces. In this work we have explored the possibility of other physical forces acting between the particles; the short range van der Waals attractive force and the force arising from interacting particles carrying a magnetic moment.

In this section, we are interested in the net displacement across streamlines caused by a collision. To represent the net streamline displacements, we plot in Fig. (8) the final absolute coordinates ($X_1^{+\infty}$, $X_3^{+\infty}$) of the incident sphere with initial positions ($X_1^{-\infty}$, $X_3^{-\infty}$) on a regular grid in $[0,3] \times [0,3]$. In this case, the particles are non-magnetic, i.e. $H_M \gg 1$. In Fig. (9) we present similar result, however, in this case, the regular grid is $[0,3.5] \times [0,3.5]$ and only the magnetic interaction effect is computed, then $H_A \gg 1$.

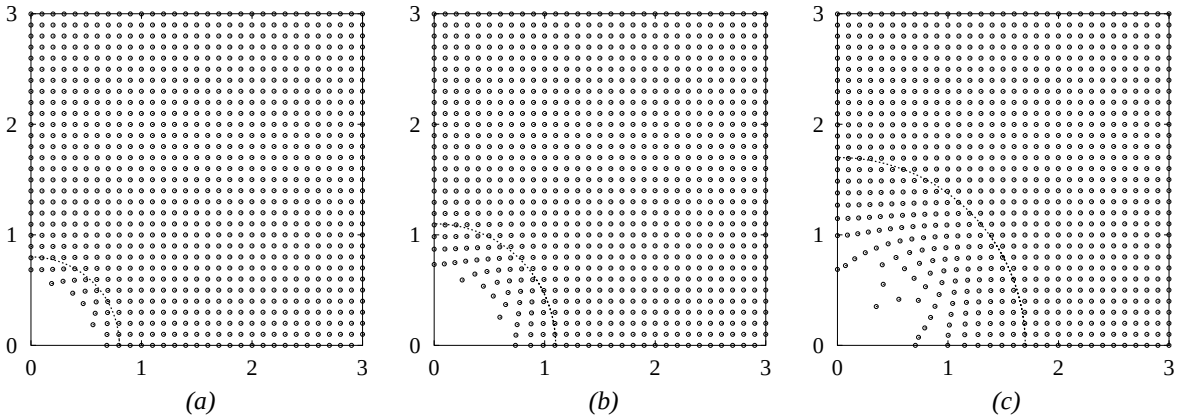

Figure 8. Reversibility diagrams for $\lambda = 0.5$, $\gamma = 1.0$ and $H_M \gg 1$. The grid points shows the distributions of final streamlines ($X_1^{+\infty}$, $X_3^{+\infty}$) for the incident sphere which started with ($X_1^{-\infty}$, $X_3^{-\infty}$). The dotted line represents the frontier between the reversible and irreversible trajectories. The different panels correspond to different values of H_A: (a) $H_A = 10.0$; (b) $H_A = 1.0$; and (c) $H_A = 0.1$.

The dotted lines in the Figs. (8) e (9) show the limit between reversible and irreversible trajectories. This boundary is defined as the all limit positions at which the difference between the transversal distances given by $\Delta X_i = |X_i^{+\infty} - X_i^{-\infty}| \leq 10^{-3}$, with $(i = 1, 3)$. This constraint was imposed based on the numerical error obtained in the simulations $\mathcal{O}(10^{-3})$. The depleted regions shown in these plots represent those trajectories that result in irreversible closed trajectories and doublet of spheres.

The heterogeneous points in the grid shown in the plots of Fig. (8) corresponds to the break of time-reversibility of the flow. We see that, when the gap between the particles decreases, the grid points are attracted for the plane origin $(X_1^{-\infty}, X_3^{-\infty}) = (0, 0)$ due to the attractive van der Waals force. Furthermore, lower values of the parameter H_A, leads to a higher density of closed trajectories and a greater probability of doublet formation. Besides, Fig. (8) also reveals that even for $H_A = 10.0$, the particles are still submitted to cross-flow migration as a consequence of the slow decayment of the van der Waals potential, i.e. $\mathcal{O}(s^{-2})$.

It is seen, in Fig. (9), that magnetic force resulting from particle interaction produces a more effective break of trajectory symmetry imposed by time-reversibility than the van der Waals attractive force. This is possible because the magnitude of the magnetic force $\mu_0 M_1^2 V_1$ is at least one order of magnitude greater than van der Waals potential energy A even with th e magnetic potential interaction ϕ_M having a more rapid decaiment $\mathcal{O}(s^{-3})$ if compared with the van der Waals potential. In particular, the results indicate that the lateral migration produced by the magnetic force is strongly dependent on the parameter H_M. The particle returns in a reversible way when the flow change its direction if hydrodynamic interactions are the only kind of interaction present in the suspension.

The diffusivity is half the rate of change in time of the variance of the displacement of the random walk. In this work, the random walk is across the streamlines and is due to collision with other particles under the gravity action. According to the theory of Cunha & Hinch (1996), we argue that the characteristic diffusivity of this mechanism is given by $D \sim \phi \, \boldsymbol{U}_{12} \, \overline{a} \, f(H_A)$, where $\overline{a} = (a_1 + a_2)/2$. The function $f(H_A)$ is obtained from an analysis of the all possible configurations of the particles for certain H_A that produce irreversible opened trajectories. In the same way, for suspensions composed of magnetic particles we propose that the dispersion coefficients of the magnetic-induced diffusion phenomenon identified here should be evaluating as being $D \sim \phi \, \boldsymbol{U}_{12} \, \overline{a} \, f(H_M)$. These diffusivity calculations certainly will be the subject of a future publication.

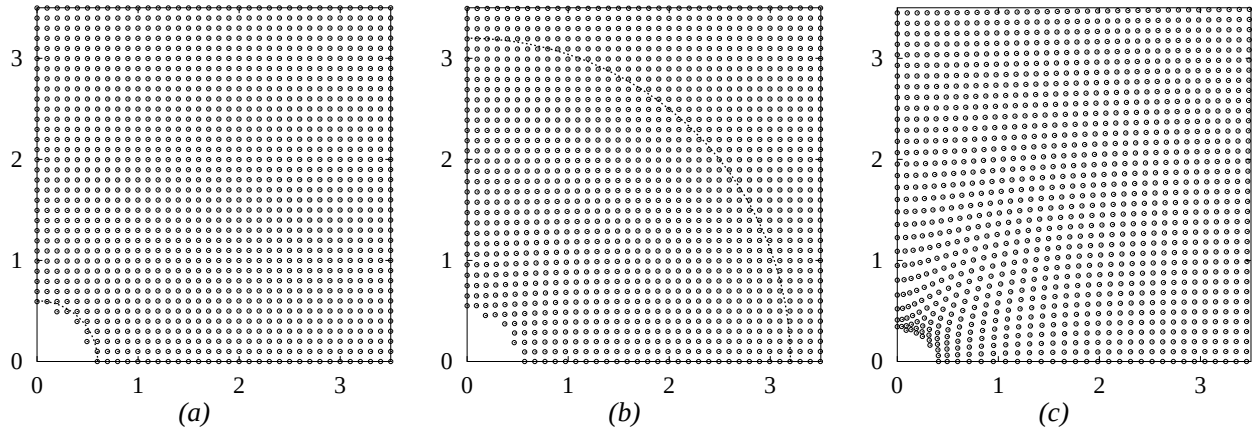

Figure 9. Reversibility diagrams for $\lambda = 0.5$, $\gamma = 1.0$ and $H_A \gg 1$. The grid points shows the distributions of final streamlines ($X_1^{+\infty}$, $X_3^{+\infty}$) for the incident sphere which started with ($X_1^{-\infty}$, $X_3^{-\infty}$). The dotted line represents the frontier between the reversible and irreversible trajectories. The different panels correspond to different values of H_M: (a) $H_M = 10.0$; (b) $H_M = 1.0$; and (c) $H_M = 0.1$.

6. Final remarks

In this article, we have developed theoretical studies on the irreversible collision of pairwise interacting particles in dilute suspensions. The computations of the particle trajectories have shown the existence of opened and closed trajectories associated with attractive van der Waals forces and magnetic force arising from the magnetization of the pair of particles. The magnetic interaction can be used as an efficient way to avoid irreversible aggregates in a suspension, promoting the suspension stabilisation. In particular, our studies has pointed out that magnetic interactions produces irreversible opened trajectories in the suspension leading to a magnetic-gravity-induced diffusion. Our next research step will compute the diffusivities in order to characterize these dispersion phenomena using the theory proposed by Cunha & Hinch (1996), comparing with those obtained from other sources of irreversibilities.

Appendix A: Expressions for the mobility functions

In this appendix, we present the asymptotic forms for the mobility functions in conditions of nearly touching spheres and widely separated spheres

A.1: Nearly touching spheres ($s < 2.3$)

$$A_{\alpha\beta} = d_{\alpha\beta}^{(1)} + d_{\alpha\beta}^{(2)}\xi + d_{\alpha\beta}^{(3)}\xi^2 \ln\xi + d_{\alpha\beta}^{(4)}\xi^2 + \mathcal{O}(\xi^2(\ln\xi)^2), \tag{21}$$

and

$$B_{\alpha\beta} = \frac{f_{\alpha\beta}^{(1)}(\ln\xi^{-1})^2 + f_{\alpha\beta}^{(2)}\ln\xi^{-1} + f_{\alpha\beta}^{(3)}}{(\ln\xi^{-1})^2 + e^{(1)}\ln\xi^{-1} + e^{(2)}} + \mathcal{O}(\xi(\ln\xi)^3), \tag{22}$$

where the geometric coefficients $d_{\alpha\beta}^{(i)}$, $f_{\alpha\beta}^{(i)}$ e $e^{(i)}$ that depends only on λ are presented by Jeffrey & Onishi (1984) and Kim & Karrila (1991).

A.2: Widely separated spheres ($s > 2.3$)

$$A_{11} = \sum_{k=0}^{\infty} f_{2k}(\lambda)(1+\lambda)^{-2k}s^{-2k} \quad \text{and} \quad A_{12} = -\frac{1}{2}(1+\lambda)\sum_{k=0}^{\infty} f_{2k+1}(\lambda)(1+\lambda)^{-2k-1}s^{-2k-1}, \tag{23}$$

where

$$f_0 = 1, \quad f_1 = -3, \quad f_2 = 0, \quad f_3 = 4 + 4\lambda^2, \quad f_4 = -60\lambda^3, \quad f_5 = 0, \quad f_6 = 480\lambda^3 - 128\lambda^5,$$

$$f_7 = -2400\lambda^3, \quad f_8 = -960\lambda^3 + 4224\lambda^5 - 576\lambda^7, \quad f_9 = 1920\lambda^3 + 1920\lambda^5,$$

$$f_{10} = -17920\lambda^5 + 96000\lambda^6 + 30720\lambda^7 - 2304\lambda^9, \quad f_{11} = -15360\lambda^3 + 231926\lambda^5 - 15360\lambda^7,$$

and

$$B_{11} = \sum_{k=0}^{\infty} f_{2k}(\lambda)(1+\lambda)^{-2k} s^{-2k} \quad \text{and} \quad B_{12} = \frac{1}{2}(1+\lambda)\sum_{k=0}^{\infty} f_{2k+1}(\lambda)(1+\lambda)^{-2k-1} s^{-2k-1}, \tag{24}$$

where

$$f_0 = 1, \quad f_1 = 3/2, \quad f_3 = 2 + 2\lambda^2, \quad f_6 = -68\lambda^5, \quad f_8 = -320\lambda^3 + 288\lambda^5 - 288\lambda^7,$$
$$f_{10} = -6720\lambda^5 + 3456\lambda^7 - 1152\lambda^9, \quad f_{11} = 8960\lambda^3 - 8848\lambda^5 + 8960\lambda^7, \quad f_2 = f_4 = f_5 = f_7 = f_9 = 0.$$

7. Acknowledgements

The authors acknowledges the financial support given by CAPES, CNPq and FINATEC.

8. References

Acrivos, A., Batchelor, G. K., Hinch, E. J., Kock, D. L. & Mauri, R., 1992, "Longitudinal shear-induced diffusion of spheres in a dilute suspension", J. Fluid Mech., Vol. 240, pp. 651.

Adler, P. M., 1981, "Interaction of unequal spheres. I. Hydrodynamic interaction: colloidal forces", J. Colloid Interface Sci., Vol. 83, pp. 83.

Couto, H. L. G., Abade, G. C. & Cunha, F. R., 2004, "Agregação e dispersão em uma suspensão coloidal de partículas interagindo hidrodinamicamente", Proceedings of the 10th Brazilian Congress of Thermal Sciences and Engineering, Vol. 1, Rio de Janeiro, 12 p.

Cunha, F. R., Almeida M. H. & Loewenberg, M., 2003, "Direct simulations of emusions flows", J. of the Braz. Soc. Mechanical Sciences, Vol. 24, pp. 1.

Cunha, F. R., 2003, "Lecture notes on Mycrohydrodynamics", Department of Mechanical Engineering, University of Brasilia.

Cunha, F. R. & Hinch, E. J., 1996, "Shear-induced dispersion in a dilute suspension of rough spheres", J. Fluid Mech., Vol. 309, pp. 211.

Curtis, A. S. G. & Hocking, L. M., 1970, "Collision efficiency of equal spherical particles in a shear flow", Trans. Faraday Soc., Vol. 66, pp. 1381.

Davis, R. H., 1984, "The rate of coagulation of a dilute polydisperse system of sedimenting spheres", J. Fluid Mech., Vol. 145, pp. 179.

Davis, R. H. & Hill, N. A., 1992, "Hydrodynamic diffusion of a sphere sedimenting throug a dilute suspension of neutrally buoyant spheres", J. Fluid Mech., Vol. 236, pp. 513.

Davis, R. H., 1992, "Effects of surface roughness on a sphere sedimenting through a dilute suspension of neutrally buoyant spheres", Phys. Fluids A, Vol. 4, No. 12, pp. 2607.

Eckstein, E. C., Bailey, D. G. & Shapiro, A. H., 1977, "Self-diffusion of particles in shear flow of a suspension", J. Fluid Mech., Vol. 79, pp. 191.

Happel, J. & Brenner, H., 1967, "Low Reynolds number hydrodynamics", Ed. Prentice-Hall, 524 p.

Kim, S. & Karrila, S. J., 1991, "Mycrohydrodynamics - Principles and Selected Applications", Ed. Butterworth - Heinemann, 507 p.

Jeffrey, D. J. & Onishi, Y., 1984, "Calculation of the resistance and mobility functions for two unequal spheres in low-Reynolds-number flow", J. Fluid Mech., Vol. 139, pp. 261.

Leighton, D. T. & Acrivos, A., 1987, "The shear-induced migration of particles in concentrated suspensions", J. Fluid Mech., Vol. 181, 415.

Lowenberg, M. & Hinch, E. J., 1997, "Collision of two deformable drops in shear flow", J. Fluid Mech., Vol. 338, pp. 299.

Rosensweig, R. E., 1985, "Ferrohydrodynamics", Ed. Dover, 344 p.

Smoluchowski, M. von, 1917, "Versuch einer mathematischen Theorie der Koagulationskinetik kolloider Lösungen", Z. Phys. Chem., Vol. 92, pp. 129.

Sobral, Y. D., Cunha, F. R., 2005, "Drift velocity and stretching of polarized drops in magnetic fields", J. Magn. Magn. Mater., Vol. 289, pp. 318.

Stratulat, R., Calugaru, G. & Badescu, V., 2000, "Magnetic carriers particles for selective separation in environmental and industrial processes", Analele Stiintifice Ale Universitatii Tomul XLV-XLVJ, s. Fizica Starii Condensate, 1999-2000, pp. 45.

Zeichner, G. R. & Schowalter, W. R., 1977, "Use of trajectory analysis to study stability of colloidal dispersions in flow fields", AlChE J., Vol. 23, pp. 243.

Zinchenko, A. Z. & Davis, R. H., 1992, "Gravity-induced coalescence of drops at arbitrary Péclet numbers", J. Fluid Mech., Vol. 280, pp. 119.

Zinchenko, A., Z., & Davis, R. H., 1994, “Collision rates of spherical drops or particles in a shear flow at arbitrary Péclet numbers”, Phys. Fluids, Vol. 7, No. 10, pp. 2310.

9. Responsibility notice

The authors are the only responsible for the printed material included in this paper.